Preparation of Titanium Dioxide/Poly(methyl methacrylate-*co*-*n*-butyl acrylate-*co*-methacrylic acid) Hybrid Composite Particles Via Emulsion Polymerization

Dong-Guk Yu,[1] Jeong Ho An,[1] Jin Young Bae,[1] Seong Deok Ahn,[2] Seung-Youl Kang,[2] Kyung Soo Suh[2]

[1]*Department of Polymer Science and Engineering, SKKU, Su-Won 440-746, Korea*
[2]*Basic Research Laboratory, ETRI, 161 Gajeong-dong, Yuseong-gu, Daejeon 305-350, Korea*

Received 17 March 2004; accepted 21 November 2004
DOI 10.1002/app.21733
Published online in Wiley InterScience (www.interscience.wiley.com).

ABSTRACT: Titanium dioxide core and polymer shell composite poly(methyl methacrylate-*co*-*n*-butyl acrylate-*co*-methacrylic acid) [P(MMA-BA-MAA)] particles were prepared by emulsion copolymerization. The stability of dispersions of TiO_2 particles in aqueous solution was investigated. The addition of an ionic surfactant, sodium lauryl sulfate, which can be absorbed strongly at the TiO_2/aqueous interface, increases the stability of the TiO_2 dispersion effectively by increasing the absolute value of the ζ potential of the TiO_2 particles. The adsorption of the nonionic surfactant, Triton X-100, on the surface of TiO_2 particles is *less* than that of the ionic surfactant. Fourier transform IR spectroscopy was used to measure the content of MAA composite particles. Dynamic light scattering characterized the composite particle size and size distribution. The field-emission scanning electron microscopy results for the composite particles showed a regular spherical shape, and no bare TiO_2 was detected on the entire surface of the samples. The composite particles that were produced showed good spectral reflectance compared to bare TiO_2. Thermogravimetric analysis results indicated the encapsulated TiO_2 and estimated density of composite particles. There was up to 78.9% encapsulated TiO_2 and the density ranged from 1.76 to 1.94 g/cm^3. The estimated density of the composite particles is suitable at 1.73 g/cm^3, which is due to density matching with the suspending fluid. The sedimentation experiment indicates that reducing the density mismatch between the composite particles and suspending fluid may enhance the stability.
 J Appl Polym Sci 97: 72–79, 2005

Key words: inorganic core; polymer shell; composite particles; emulsion polymerization; encapsulation efficiency

INTRODUCTION

Encapsulated particles consisting of an inorganic core and a polymer shell are of interest in various applications, such as cosmetics, inks, and pants, because of their better mechanical properties and the dispersion stability of the suspending medium.[1–3] Electronic papers have recently been of great interest for applications in information displays requiring low cost, low weight, flexibility, and low power consumption. The displays with these requirements can be achieved by methods using cholesteric liquid crystals, twisting balls, mobile fine particles with liquid crystals, in-plane electrophoretic particles, and microencapsulated electrophoretic particles. For the image retaining property of the electrophoretic displays (EPDs), the pigment particles should be well dispersed in the low dielectric suspending medium for a long time and agglomeration of the particles should be prohibited. TiO_2 particles are the most promising white pigments for EPDs, because of their excellent whiteness. However, their density (ρ) is nearly 4.2 g/cm^3, which is so high that a polymer coating is necessary for the density matching with the usual low dielectric suspending fluid (ρ = 1.73 g/cm^3). In recent literature, several processes have been described to synthesize particles that consist of an inorganic core surrounded by a polymer shell.[4–6] Bakhshaee et al. used a suspension polymerization approach to encapsulate carbon black for toner production and Cooper and Vincent described the encapsulation of silica particles in poly(methyl methacrylate) beads.[7,8] Caris et al. have used TiO_2 particles modified with a titanate coupling agent.[9] Such modified particles have strong bonds with the particle, although the alkoxy group is able to react with the surface hydroxyl groups of the particle, and with the unsaturated group, which is able to participate in the radical polymerization. Lorimer and Templeton-Knight tried to encapsulate TiO_2 particles by using ultrasonic cavitations.[10,11] These authors did carry out the emulsion polymerization using ultrasonic stirring during the first steps of the process.

Correspondence to: D.-G. Yu (polyyoo@skku.edu).
Contract grant sponsor: Korea Ministry of Information and Communications.

Journal of Applied Polymer Science, Vol. 97, 72–79 (2005)

TABLE I
Recipes for Emulsion Polymerization of TiO_2/P(MMA-BA-MAA) Composite

		Monomer			Surfactant			
Sample ID	TiO_2 (g)[a]	MMA (g)	BA (g)	MAA (g)	SLS (g)	Triton X-100 (g)	APS (mg)[b]	DI water (g)
TPMA-5	4	6	0.6	0.3	0.25	0.08	69	400
TPMA-10	4	6	0.6	0.6	0.25	0.08	72	400
TPMA-15	4	6	0.6	0.9	0.25	0.08	75	400

TPMA, TiO_2/P(MMA-BA-MAA); APS, ammonium persulfate.
[a] 1 wt % of reaction medium.
[b] 1 wt % of total monomer.

Much more recently, the encapsulation of TiO_2 in miniemulsion polymerization of styrene was discussed.[12–14] In the present study, we describe a rather simple encapsulation procedure of TiO_2 particles based on emulsion polymerization of acrylic monomers. The inorganic/organic composite particles are produced by coupling already existing polymer chains to the *inorganic* surface or polymerizing in the interface of the inorganic particles. The dispersion stability of TiO_2 in the monomer mixture is crucially dependent on the surface characteristics of TiO_2 in the dispersion state during polymerization. In this contribution, the usefulness of emulsion polymerization in producing carboxylic acid functional group titanium dioxide/poly(methyl methacrylate-*co*-*n*-butyl acrylate-*co*-methacrylic acid) [TiO_2/P(MMA-BA-MAA)] hybrid composite particles was estimated considering the composite particles. Finally, their spectral reflectance and density were estimated to find an appropriate application in EPDs.

EXPERIMENTAL

Materials

MMA and BA (Sigma–Aldrich Co. Ltd) were chemically pure grade and purified by reduced pressure distillation. MAA was used as shipped. Ammonium persulfate was purified by recrystallization. Commercial product grade sodium lauryl sulfate (SLS) and Triton X-100 were used without further purification. TiO_2 (R-900, DuPont Ti-Pure) pigment particles with an average particle size 0.42 μm were used as core materials. Poly(chlorotrifluoroethylene) oil (DP = 4–10, Halocarbon Product Corp., River Edge, NJ) was used as a suspending fluid (ρ = 1.73 g/cm^3). All other chemicals were reagent grade.

Polymerization procedure

Emusifiers (SLS and Triton X-100) and inorganic TiO_2 dispersed in the aqueous phase were introduced into the reaction flask, heated to 70°C, and stirred at a rate of 250 rpm. Nitrogen gas was bubbled through the solution for deoxygenation. After 30 min, ammonium persulfate and the monomer mixture were poured into the reaction flask. The pH of the reactant mixture was adjusted by the addition of HCl or NaOH solution. The reaction was then allowed to polymerize for 24 h under the constant stirring rate. Cooling to room temperature terminated the reaction. The reaction mixture of the encapsulating composite particles was separated by ethyl ether (to remove the unreacted monomer). The supernatant was decanted and the remaining pigment/polymer composite particles were washed 5 times with deionized water. Finally, the pigment/polymer composite particles were dried at −90°C in a freeze drier. The representative recipe and the reaction parameters investigated in this study are shown in Table I. Here, TiO_2/P(MMA-BA-MAA) hybrid composite particles are symbolized by TPMA-α, where α represents the percent weight fraction of MAA.

Characterization

The ζ potential of TiO_2 was calculated according to the Smoluchowski equation, $\zeta = 4\pi\eta U/\varepsilon$ (where ε is the permittivity and η is the viscosity), for a velocity of electrophoresis (U) that was measured by the microscopic electrophoresis method using a ζ-potential analyzer (Zetasizer 2000, Malvern). Fourier transform IR spectrophotometry (FTIR) was used to characterize the functional groups of the pigment/polymer composite particles. The pigment/polymer composite sample was ground with dried potassium bromide (KBr) powder and compressed into a disk. The KBr disk was subjected to analysis by an IR spectrophotometer. The particle size and particle size distribution were measured by dynamic light scattering (DLS, Brookhaven). The samples for DLS were prepared by dilution with methanol. The surface morphology was observed using field-emission scanning electron microscopy (FE-SEM, Hitachi S-4300). Powder X-ray diffraction (XRD) spectra patterns were obtained with a MAC Science M18 X-ray diffractometer (100 kV, 200 mA) with CuKα and Ni filters with a wavelength of

0.154 nm at a scanning rate of 3°/min. The 2θ values ranged from 10° to 80°. The spectral reflectance of the samples was measured relative to a zinc oxide (ZnO) standard plate. In order to evaluate the thermal properties, coating efficiency, and density of the inorganic/polymer hybrid composite particles, a thermal analysis was performed for the powder of the composite materials obtained in a freeze drier for 3 days. Samples of 10–30 mg of powder were put into a gold crucible for thermogravimetric analysis (TGA). The heating rate was 10°C/min in nitrogen gas. The recorded temperature range was from 50 to 650°C. The encapsulated TiO_2 (E_{TiO2}) and experimental density of the composite particles was determined by incineration of the polymer shell using TGA. The percentage of TiO_2 encapsulated was calculated as follows:

$$E_{TiO2} = (\text{residual weight of } TiO_2 \text{ after incineration})/(\text{theoretical weight of } TiO_2 \text{ in samples}) \times 100 \quad (1)$$

where the theoretical weight of TiO_2 is defined as

$$\text{theoretical weight of } TiO_2 = (\text{weight of dried sample}) \times (\text{weight fraction of } TiO_2 \text{ in the sample}) \quad (2)$$

$$\text{theoretical weight fraction of } TiO_2 = (\text{weight of } TiO_2)/(\text{weight of polymer} + \text{weight of } TiO_2) \quad (3)$$

$$\text{density } (g/cm^3) = 4.1 \times (\text{weight fraction of } TiO_2 \text{ in dried sample}) + 1.1 \times (\text{weight fraction of polymer}) \quad (4)$$

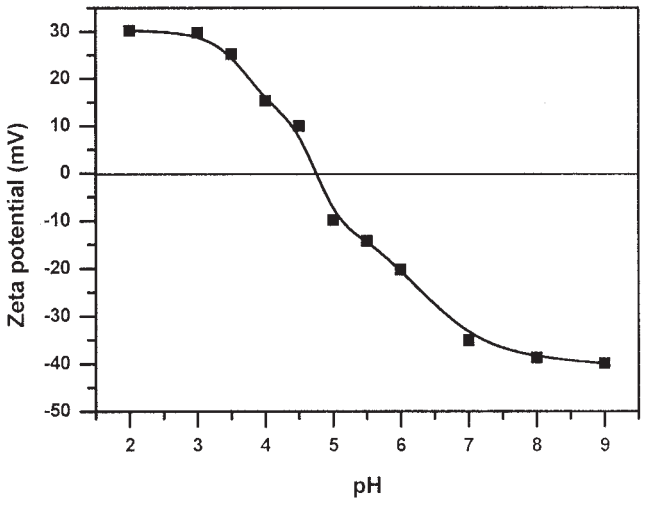

Figure 1 The relation between the ζ potential of TiO_2 R-900 and the hydrogen ion concentration.

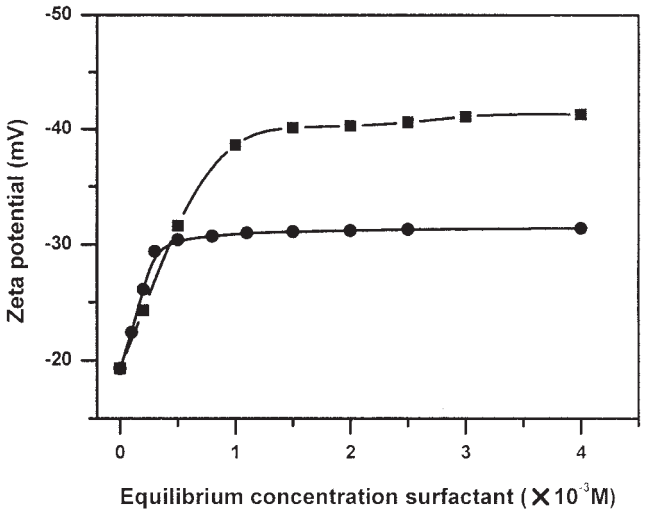

Figure 2 Variations of the ζ potential versus the (■) ionic and (●) nonionic surfactants for the aqueous dispersions of the TiO_2 particles.

The stability and density match was evaluated for the composite TiO_2 particles by measuring the sedimentation height of the composite particles dispersion with a solid content of 2 wt % of the suspending fluid (ρ = 1.73 g/cm^3).

RESULTS AND DISCUSSION

The relationship between the ζ potential of TiO_2 and the pH of the polymerization mixture is shown in Figure 1. When the pH of the reaction mixture was adjusted by the addition of HCl or NaOH solution, the TiO_2 was positively charged with an increase in the HCl concentration and negatively charged with an increase in the NaOH concentration. TiO_2 is negatively charged near neutrality because its isoelectric point is pH 4.7. Haga et al. reported that the inorganic and the growing polymer have opposite charges: a polymer shell formed around the inorganic particles.[15] For encapsulation polymerization, therefore, the electrostatic interaction between the surface charge of TiO_2 and the charge of the monomer is considered to be in the earlier stage of polymerization.

Figure 2 presents the adsorption of SLS and Triton X-100 on the TiO_2 particles dispersed in 0.05*M* NaCl solution with a pH value of 6.0. It can be seen from Figure 2 that the adsorption isotherms of both SLS and Triton X-100 reach a plateau at about (1.5 and 0.5) $\times 10^{-3}$ *M*, respectively. The results shown in Figure 2 clearly indicate that SLS may be absorbed strongly on the surface of TiO_2 particles, although the surface active anions on SLS and the surface of the TiO_2 particles are both negatively charged under the experimental conditions. Because the surface of TiO_2 is generally strongly hydrated, the mechanism of the bind-

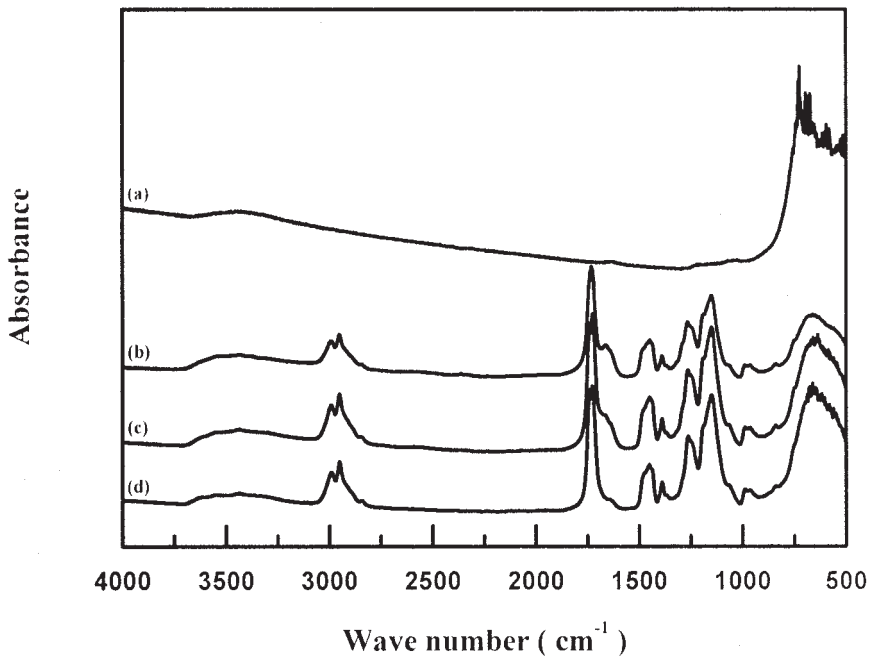

Figure 3 FTIR spectra of bare TiO_2 (spectrum a), TPMA-5 (spectrum b), TPMA-10 (spectrum c), and TPMA-15 (spectrum d).

ing of the initial surface active anions on the negatively charged surface is somewhat hard to absorb. One possible interpretation is that two types of hydroxyl groups exist on the surface of TiO_2, one type bound to one terminal hydroxyl group and the other to two bridged hydroxyl groups. The bridged group should be strongly polarized by the cations and therefore be acidic, whereas the terminal hydroxyl group should be predominantly basic and exchangeable with other anions. According to this model, the basic hydroxyl groups may exchange with other anions of the SLS solution, leading to the adsorption of the initial surface active anions on the TiO_2 surface. Figure 2 also shows the adsorption isotherm of a nonionic surfactant, Triton X-100, on the TiO_2 particles and the corresponding variation of the ζ potential. It can be seen that the adsorption of TiO_2 is weaker, having a saturated adsorption amount that is 33% of that of SLS. The ζ potential is only slightly increased by adsorption of the uncharged Triton X-100. It appears that the nonionic surfactant lacks an attraction with the solid surface that is sufficient to overcome the strong interaction between the ethylene oxide group and the water to be absorbed.

The FTIR spectroscopy results for the samples are shown in Figure 3. Figure 3(a) corresponds to the TiO_2 raw material and Figure 3(b–d) correspond to the TPMA-5, TPMA-10, and TPMA-15 composite particles, respectively. The vibration absorption shows at low frequencies, such as 800 cm^{-1}, the existence of a Ti—O—Ti backbone. The region around 3400–3600 cm^{-1} has characteristic peaks for hydroxyls on the TiO_2 particle surface [Fig. 3(a)]. In the spectra of the Figure 3(c,d) samples, the functional group is observed through the presence of bands in the region of 1680–1730 cm^{-1} that belong to C═O asymmetric and symmetric vibrations of the carboxylic acid. The bands at 1236 and 1100 cm^{-1} are attributed to the vibration of the C—O—C bands, whose identification with FTIR spectroscopy has already been described. In Figure 3(c,d), it is possible to observe a broad band region of 3300–3600 cm^{-1} that is associated with the hydroxyl groups. The bands in the 2800–3000 cm^{-1} region corresponds to the CH_2 and CH_3 groups of the polymer backbone. The bands at 1730 cm^{-1} are assigned to the

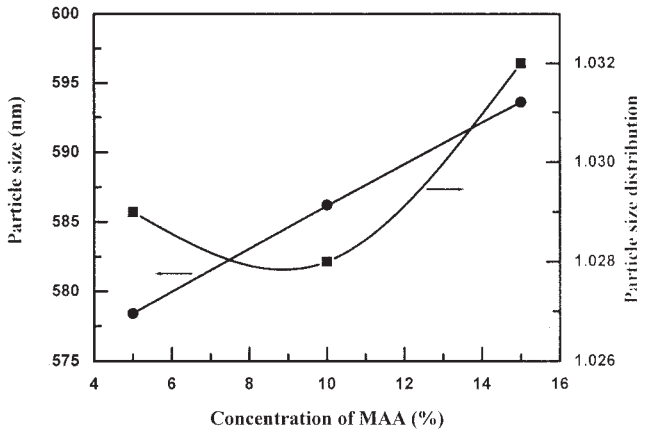

Figure 4 The (●) mean particle size and (■) particle size distribution of composite particles versus the MAA concentration.

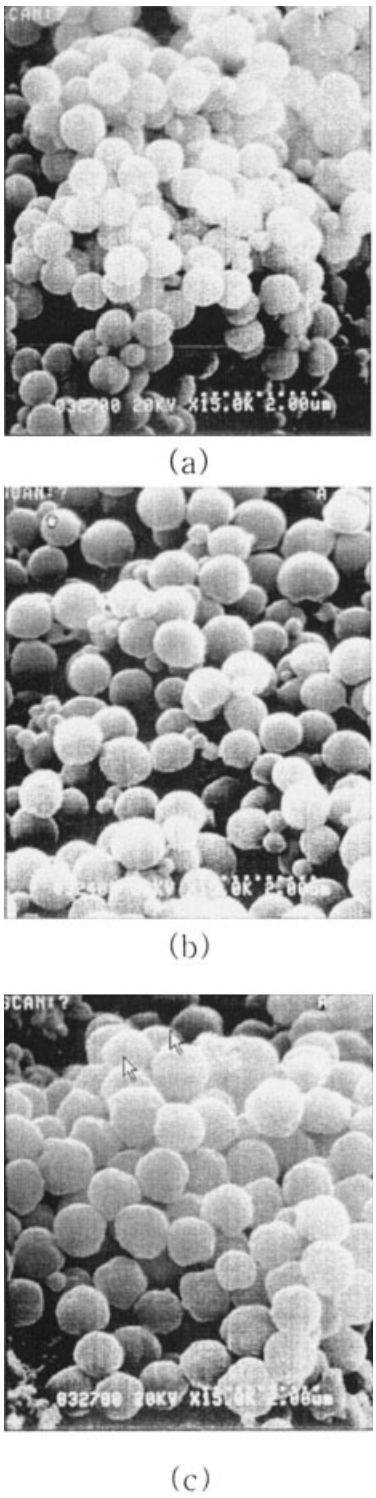

Figure 5 FE-SEM micrographs of (a) TPMA-5, (b) TPMA-10, and (c) TPMA-15.

symmetric C═O stretch of the carboxylic acid. In addition, the region of bands at 500–800 cm^{-1} is tentatively assigned to Ti—O—Ti groups. The above results of the FTIR spectra proves the formation of the composite particles.

The particle size and particle size distributions were determined, as shown in the Figure 4. The average particle size of the composite particles ranged from 578.4 to 593.6 nm. The particle size distribution had narrow distributions in most cases, but it was relatively narrower than bare TiO_2. There is no MAA in the reaction in the early nucleation stage when MAA is added in the latter nucleation stage. The average particle diameter of TPMA-15 is larger than TPMA-5. MAA is mainly located at the surface of the composite particles, so the average particle diameter increases with increasing concentration of monomer.

Figure 5 shows an FE-SEM image of composite particles. From this observation one can deduce that the bare TiO_2 particles encapsulated during the polymerization, embedded in the polymer, or became more anchored in the polymer. The surface of the composite particles was smooth and had a regular spherical shape, and no bare TiO_2 particles were detected on the entire surface of the samples. Figure 6 contains the XRD patterns of bare TiO_2 and TPMA-α composite particles. In Figure 6(a), the bare TiO_2 diffraction patterns reveal three main peaks with 2θ values of 27.4°, 35.9° and 41.3°, corresponding to rutile TiO_2. In Figure 6(b–d), the broad peak between 15° and 25° is assigned to amorphous acrylic polymer.

Figure 7 and Figure 8 show TGA thermograms obtained from the bare TiO_2, P(MMA-BA-MAA) reference, and composite samples. Obviously, the onset temperatures of thermal decomposition shown by those composites [Fig. 8(b–d)] are shifted toward a higher temperature range than that of the reference polymer [Fig. 8(b)], indicating the enhancement of the thermal stability of the composite samples. It is noticeable that the composites are showing the onset tem-

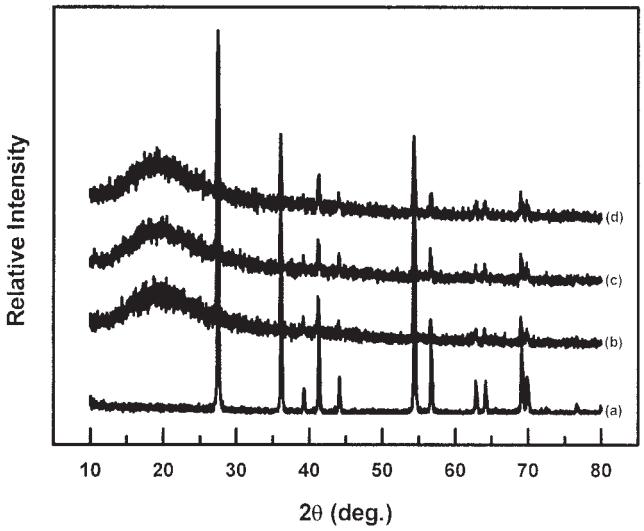

Figure 6 X-ray diffractograms of bare TiO_2 (spectrum a), TPMA-5 (spectrum b), TPMA-10 (spectrum c), and TPMA-15 (spectrum d).

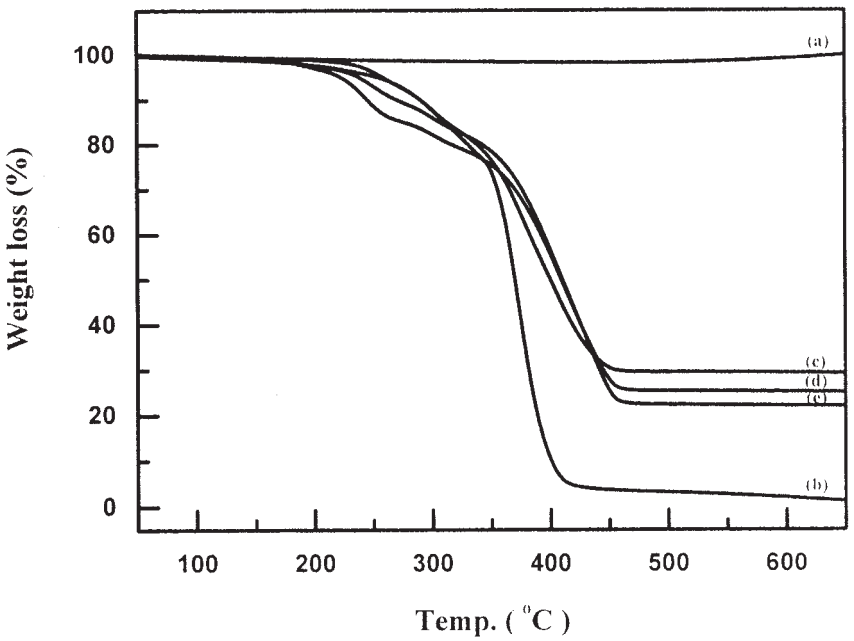

Figure 7 TGA thermograms of bare TiO_2 (spectrum a), P(MMA-*co*-BA) reference (spectrum b), TPMA-5 (spectrum c), TPMA-10 (spectrum d), and TPMA-15 (spectrum e).

peratures of 386.8, 410.1, and 408.1°C as their polymer content increases. Table II also provides the encapsulation efficiency and estimated density of the TPMA-α composite samples. In general, the encapsulation efficiency depended on the ratio of core materials (TiO_2/polymer shell polymer). TPMA-α was used as the encapsulating polymer (TPMA-5, TPMA-10, and TPMA-15 TiO_2/TPMA-α ratios = 1:1.65, 1:1.725, and 1:1.8), and the encapsulated TiO_2 ranged from 61.7 to 78.9% of TiO_2 in the oil phase being encapsulated. The

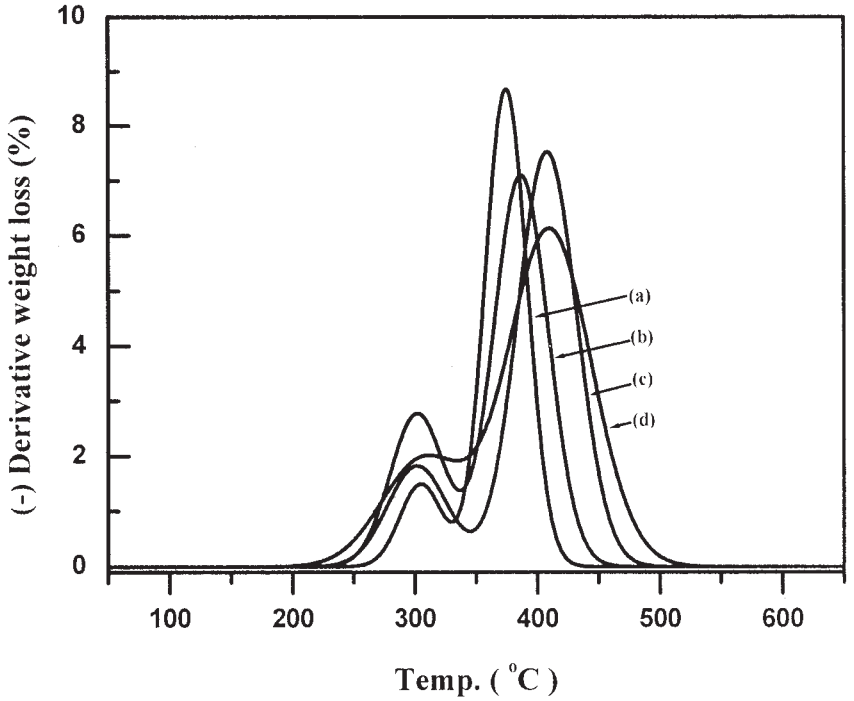

Figure 8 The derivative weight loss of the P(MMA-*co*-BA) reference (spectrum a), TPMA-5 (spectrum b), TPMA-10 (spectrum c), and TPMA-15 (spectrum d).

TABLE II
TGA Thermograms, Encapsulation Efficiency, and Density of TPMA-α Composite Samples

Sample ID	Weight (mg)		Decomp. onset temp.[a]	Encapsul. TiO_2 (%)	Estim. density (g/cm^3)	Theor. density (g/cm^3)
	Initial	Final				
TiO_2	20.32	20.38	—	—	—	4.1
Polymer[b]	20.85	0.17	374.7	—	—	1.06[c]
TPMA-5	14.48	4.19	386.8	78.9	1.94	2.21
TPMA-10	15.63	3.91	410.1	70.0	1.82	2.18
TPMA-15	13.85	3.05	408.1	61.7	1.76	2.15

[a] Main maximum decomposition temperature.
[b] P(MMA-BA).
[c] Density of PMMA.

encapsulated TiO_2 was decreased when increasing the concentration of MAA. In addition, the estimated density was decreased when increasing the concentration of MAA. The density of the composite samples ranged from 1.76 to 1.94 g/cm^3. The estimated density was lower than the theoretical density. The lower encapsulated TiO_2 and estimated density of the higher concentration of MAA probably resulted from the escape of TiO_2 particles entrapped inside the droplets into continuous phase.

The spectral reflectance of ZnO, bare TiO_2, and composite samples are shown in Figure 9. Compared with the bare TiO_2, all the composite samples displayed slightly low spectral reflectance. This happens because the polymer shell of the composite samples is protected from the penetration of UV. However, the polymer shell thickness is about 200 nm, and UV light penetrates the polymer shell. Thus, all the composite samples show nearly the same spectral reflectance as bare TiO_2. As shown in the Figure 10, the encapsulated particles in our hybrids endow their suspensions with excellent sedimentation stability. As the density of the composite particles decreases, its suspension stability is also augmented. The composite particles do not deposit for 2 weeks, whereas TiO_2 particles completely deposit in 2 days. Reducing the density mismatch between the composite particles and the suspending fluid may enhance the stability.

CONCLUSION

Emulsion polymerization was used to prepare TiO_2 core and P(MMA-BA-MAA) shell hybrid composite particles. The addition of surfactants (SLS and Triton X-100),

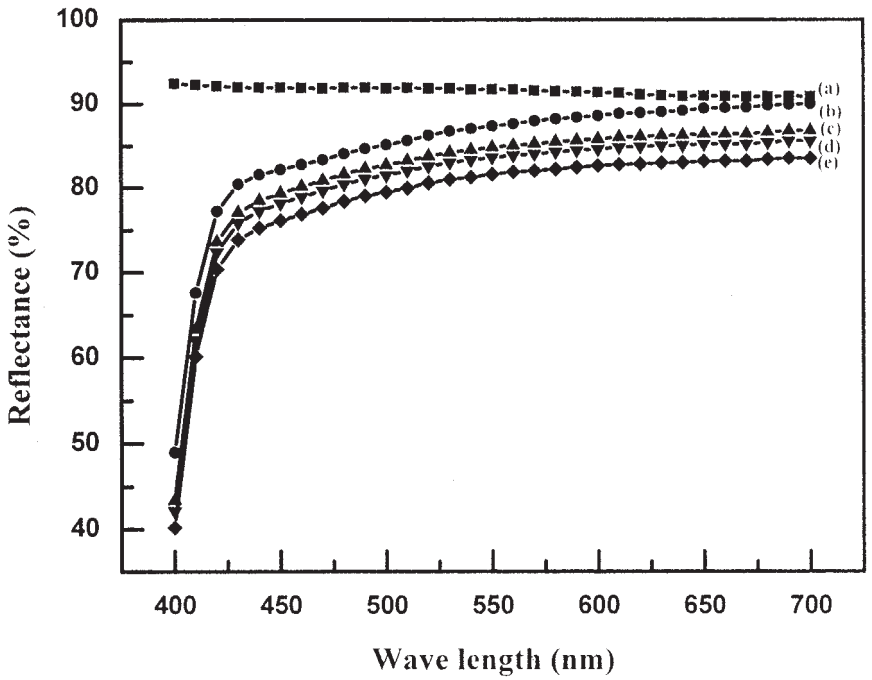

Figure 9 The spectral reflectance of the ZnO standard (spectrum a), bare TiO_2 (spectrum b), TPMA-5 (spectrum c), TPMA-10 (spectrum d), and TPMA-15 (spectrum e).

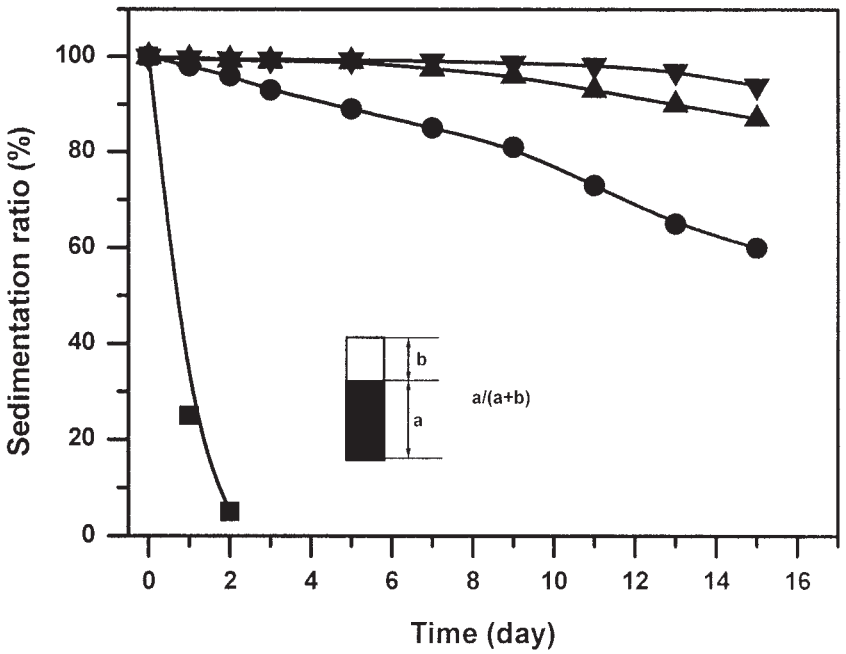

Figure 10 The sedimentation ratio of the TiO_2/polymer composite vs. time; (●) TPMA-5, (△) TPMA-10, (▼) TPMA-15, and (■) TiO_2.

which can be absorbed at the TiO_2/solution interface, effectively increases the stability of the TiO_2 dispersion by increasing the value of the ζ potential of the TiO_2 particles. The presence of carboxylic acid groups on the composite particles was confirmed by FTIR. The DLS and FE-SEM results of the composite particles showed a narrow size distribution and regular spherical shape and no bare TiO_2 particles detected on the whole surface of the samples, respectively. XRD patterns of the broad bands reflected the amorphous polymer composite. The TGA results indicated the encapsulation efficiency and density of the composite particles. There was up to 78.9% encapsulated TiO_2 and the estimated density ranged from 1.76 to 1.94 g/cm^3. The estimated density of the composite TiO_2 particles was suitable at 1.73 g/cm^3, which was due to density matching with the suspending media. The UV results showed that the decrease in the spectral reflectance values was negligibly small; it is believed that the composite samples will not cause any problems in their ultimate uses. In further applications, they are expected to find great usefulness in EPDs.

The Korea Ministry of Information and Communications financially supported this work.

References

1. Haga, Y.; Inoue, S.; Saito, T.; Yoshimiya, R. Angew Macromol Chem 1986, 139, 49.
2. Caris, C. H. M.; Kuijpers, R. P. M.; Heck, A. M.; German, A. C. Macromol Symp 1990, 35, 335.
3. Hasegawa, M.; Arai, K.; Saito, S. J Polym Sci Part A: Polym Chem 1987, 25, 3231.
4. Sellergren, B.; Dauwe, C.; Schneider, T. Macromolecules 1997, 30, 2454.
5. Landfester, K. Macromol Rapid Commun 2001, 22, 896.
6. Erdem, B.; Sudol, E.; Dimonie, V. L.; El-Aasser, M. S. J Polym Sci Part A: Polym Chem 2000, 38, 4419.
7. Bakhshaee, M.; Pethrick, R. A.; Rashid, H.; Sherrington, D. C. Polymer 1985, 26, 185.
8. Cooper, E. C.; Vincent, B. J. Colloid Interface Sci 1989, 132, 592.
9. Caris, C. H. M.; Elven, L. P. M.; Herk, A. M.; German, A. L. Br Polym J 1989, 21, 133.
10. Lorimer, J. P.; Templeton-Knight, R. Colloid Polym Sci 1991, 269, 392.
11. Templeton-Knight, R. L. J Oil Color Chem Assoc 1990, 73, 459.
12. Pal, J.; Baydal, S.; Templeton-Knight, R. J Chem Soc Faraday Soc 1991, 87, 991.
13. Erdem, B.; Sudol, E.; Dimonie, V. L.; El-Aasser, M. S. J Polym Sci Part A: Polym Chem 2000, 38, 4431.
14. Erdem, B.; Sudol, E.; Dimonie, V. L.; El-Aasser, M. S. J Polym Sci Part A: Polym Chem 2000, 38, 4441.
15. Haga, Y.; Watanabe, T. Angew Makromol Chem 1991, 188, 73.